Molecular Engineering of Liquid Crystalline Polymers by Living Polymerization. 10. Influence of Molecular Weight on the Phase Transitions of Poly{ω-[(4-cyano-4′-biphenylyl)oxy]alkyl vinyl ether}s with Nonyl and Decanyl Alkyl Groups

Virgil Percec* and Myongsoo Lee

Department of Macromolecular Science, Case Western Reserve University, Cleveland, Ohio 44106

Received October 15, 1990; Revised Manuscript Received December 4, 1990

ABSTRACT: The synthesis and living cationic polymerization of 9-[(4-cyano-4′-biphenyl)oxy]nonyl vinyl ether (**6–9**) and 10-[(4-cyano-4′-biphenylyl)oxy]decanyl vinyl ether (**6–10**) are described. The mesomorphic behavior of poly(**6–9**) and poly(**6–10**) with narrow molecular weight distributions and degrees of polymerization from 2 to 32 was discussed by comparison to that of 9-[(4-cyano-4′-biphenylyl)oxy]nonyl ethyl ether (**8–9**) and 10-[(4-cyano-4′-biphenylyl)oxy]decanyl ethyl ether (**8–10**), which are the model compounds of the monomeric structural units of poly(**6–9**) and poly(**6–10**). **8–9** exhibits monotropic nematic and monotropic s_A, while **8–10** exhibits monotropic smectic A mesophases. Irrespective of the thermal history of the sample, over the entire range of molecular weights, poly(**6–9**) exhibits an enantiotropic s_A mesophase. In the first heating scan, poly(**6–10**) exhibits a crystalline phase followed by an enantiotropic s_A mesophase. In the second heating scan, poly(**6–10**)s with degrees of polymerization below 16 exhibit an enantiotropic s_A mesophase, while polymers with higher degrees of polymerization display both s_A and s_X (unidentified) enantiotropic mesophases. Finally, the phase behavior of poly{ω-[(4-cyano-4′-biphenylyl)oxy]alkyl vinyl ether}s with alkyl from ethyl to undecanyl will be discussed at four different degrees of polymerization: 30, 23, 13, and 4.

Introduction

The dependence of phase transition temperatures on polymer molecular weight represents the most elementary relationship that should be elucidated in order to provide a systematic approach to the molecular engineering of side-chain liquid crystalline polymers. The only trend that is generally accepted consists of the enlargement of the temperature range of the mesophase that occurs with the increase of the polymer molecular weight.[1-15] The transition from monomer to polymer can also generate the transformation of a virtual or monotropic mesophase of the monomeric structural unit or of the monomer into a monotropic or enantiotropic one. This dependence was recently explained on the basis of thermodynamic principles assuming that the behavior of the polymer is determined by that of the monomeric structural unit.[16,17] However, there are several reports that have demonstrated that the number of mesophases and the nature of the mesophase both change by increasing the molecular weight of the polymer.[4,5,7-15] Although, at the first sight, this trend seems "unexpected", it was already confirmed for several different polymer systems.

Consequently, the first goal of this series of publications is to provide a complete elucidation of the influence of molecular weight on the phase behavior of poly{ω-[(4-cyano-4′-biphenylyl)oxy]alkyl vinyl ether}s containing alkyl groups from ethyl to undecanyl. We decided to investigate this particular series of polymers because their corresponding monomers can be polymerized through a living cationic polymerization mechanism, and, therefore, polymers with well-defined molecular weights and narrow molecular weight distributions can readily become available.[11-15] The initiating system that we prefer to use in these polymerizations is $CF_3SO_3H/(CH_3)_2S$.[18]

* To whom all correspondence should be addressed.

The goal of this paper is to describe the synthesis and living cationic polymerization of the last two monomers from this series, i.e., 9-[(4-cyano-4′-biphenylyl)oxy]nonyl vinyl ether (**6–9**) and 10-[(4-cyano-4′-biphenylyl)oxy]decanyl vinyl ether (**6–10**). The influence of molecular weight on their phase transitions will be discussed by comparison to that of 9-[(4-cyano-4′-biphenylyl)oxy]nonyl ethyl ether (**8–9**) and 10-[(4-cyano-4′-biphenylyl)oxy]decanyl ethyl ether (**8–10**), which represent the model compounds of the monomeric structural units of poly(**6–9**) and poly(**6–10**). Then the mesomorphic behavior of poly{ω-[(4-cyano-4′-biphenylyl)oxy]alkyl vinyl ether}s with alkyl groups containing from 2 to 11 methylenic units will be comparatively discussed at four different degrees of polymerization: 30, 23, 13, and 4. The implication of different phase transitions at various molecular weights on the molecular design of novel macromolecular architectures based on side-chain liquid crystalline polymers is briefly discussed.

Experimental Section

Materials. 4-Phenylphenol (98%), 1,10-phenanthroline (anhydrous, 99%), palladium(II) acetate (all from Lancaster Synthesis), ferric chloride anhydrous (98%, Fluka), copper(I) cyanide (99%), 9-borabicyclo[3.3.1]nonane (9-BBN, crystalline, 98%), 9-bromononan-1-ol (97%), 10-bromodecan-1-ol (90%), and the other reagents (all from Aldrich) were used as received. Methyl sulfide (anhydrous, 99%, Aldrich) was refluxed over 9-BBN and then distilled under argon. Dichloromethane (99.6%, Aldrich) used as a polymerization solvent was first washed with concentrated sulfuric acid and then with water, dried over anhydrous magnesium sulfate, refluxed over calcium hydride, and freshly distilled under argon before each use. *N*-methyl-2-pyrrolidone (98%, Lancaster Synthesis) was dried by azeotropic distillation with benzene, shaken with barium oxide, filtered, and fractionally distilled under reduced pressure. Trifluoromethanesulfonic acid (triflic acid, 98%, Aldrich) was distilled under argon.

0024-9297/91/2224-2780$02.50/0

Scheme I
Synthesis of 9-[(4-Cyano-4′-biphenylyl)oxy]nonyl Vinyl Ether (6–9) and 7-[(4-Cyano-4′-biphenylyl)oxy]heptyl Vinyl Ether (6–10) and Model Compounds 8–9 and 8–10

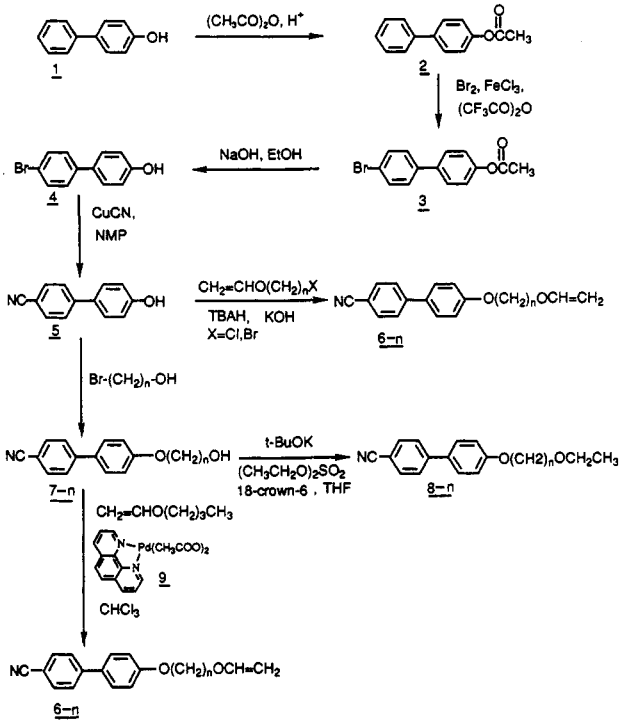

Techniques. ^{1}H NMR (200 MHz) spectra were recorded on a Varian XL-200 spectrometer. TMS was used as internal standard. A Perkin-Elmer DSC-4 differential scanning calorimeter, equipped with a TADS 3600 data station, was used to determine the thermal transitions that were reported as the maxima and minima of their endothermic or exothermic peaks, respectively. In all cases, heating and cooling rates were 20 °C/min unless otherwise specified. Glass transition temperatures (T_g) were read at the middle of the change in the heat capacity. For certain polymer samples, first heating scans sometimes differ from second and subsequent heating scans. At the proper place, this difference will be discussed. However, second and subsequent heating scans are identical. Although in the present case both sets of data are identical, they will be reported. A Carl-Zeiss optical polarized microscope (magnification 100x) equipped with a Mettler FP 82 hot stage and a Metter FP 800 (magnification 100x) equipped with a Mettler FP 82 hot stage and a Metter FP 800 central processor were used to observe the thermal transitions and to analyze the anisotropic textures.[19,20] Molecular weights were determined by gel permeation chromatography (GPC) with a Perkin-Elmer series 10 LC instrument equipped with an LC-100 column oven, an LC-600 autosampler, and a Nelson analytical 900 series integrator data station. The measurements were made at 40 °C with the UV detector. A set of Perkin-Elmer PL gel columns of 10^4 and 500 Å with $CHCl_3$ as solvent (1 mL/min) and a calibration plot constructed with polystyrene standards was used to determine the molecular weights. High-pressure liquid chromatography (HPLC) experiments were performed with the same instrument.

Synthesis of Monomers. Scheme I outlines the synthesis of monomers and model compounds, while Scheme II shows the polymerization reaction.

(1,10-Phenanthroline)palladium(II) Diacetate (9). (1,10-Phenanthroline)palladium(II) diacetate was synthesized according to a literature procedure,[21] mp 235–236 °C (ref 21, mp, 234 °C).

4-Cyano-4′-hydroxybiphenyl (5). 5 was synthesized as reported in a previous publication.[11,22] Purity, 99% (HPLC); mp 195–198 °C (refs 20 and 21, mp 196–199 °C); ^{1}H NMR (acetone-d_6, TMS, ppm) δ 3.80 (1 proton, OH, s), 7.01 (2 aromatic protons, ortho to OH, d), 7.61 (2 aromatic protons, meta to OH, d), 7.70 (4 aromatic protons, ortho and meta to CN, s).

Scheme II
Cationic Polymerization of 6–9 and 6–10

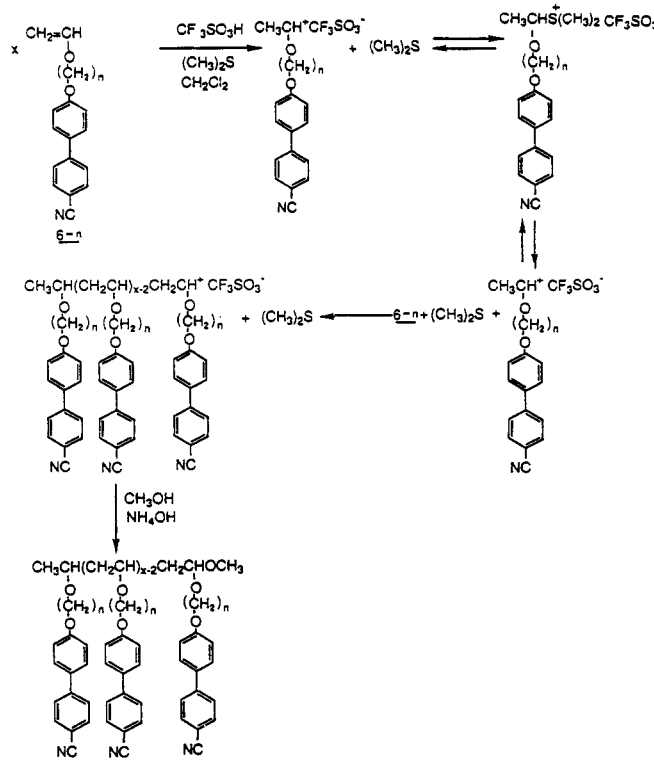

Synthesis of 4-Cyano-4′-[(9-hydroxynonan-1-yl)oxy]biphenyl (7–9). 4-Cyano-4′-hydroxybiphenyl (4.37 g, 0.0224 mol) and potassium carbonate (9.29 g, 0.067 mol) were added to a mixture of acetone–DMSO (10.1) (110 mL). 9-Bromononan-1-ol (5 g, 0.0224 mol) was added to the resulting solution, which was heated to reflux for 24 h. After it cooled, the mixture was poured into water and then filtered. The obtained solid was recrystallized from methanol and then benzene, to yield 5.6 g (74.1%) of white crystals. Mp 81.4 °C; T_{n-i}, 98.9 °C (DSC); ^{1}H NMR ($CDCl_3$, TMS, ppm) δ 1.01–1.95 (14 protons, $(CH_2)_7$, m), 3.65 (2 protons, CH_2OH, t), 4.00 (2 protons, $PhOCH_2$, t), 7.00 (2 aromatic protons, ortho to alkoxy, d), 7.51 (2 aromatic protons, meta to alkoxy, d), 7.66 (4 aromatic protons, ortho and meta to CN, d of d).

4-Cyano-4′-[(9-hydroxynonan-1-yl)oxy]biphenyl (4.0 g, 0.012 mol) was added to a mixture of (1,10-phenanthroline)palladium-(II) diacetate (0.48 g, 1.2 mmol), *n*-butyl vinyl ether (64.6 mL) and dry chloroform (17.1 mL). The mixture was heated to 60 °C for 6 h. After it cooled, it was filtered to remove the catalyst and the solvent was distilled in a rotavapor. The product was purified by column chromatography (silica gel, CH_2Cl_2 eluent) and then recrystallized from *n*-hexane to yield 3.6 g (83.6%) of white crystals. Purity, 99.6% (HPLC); mp 63.1 °C (DSC); ^{1}H NMR ($CDCl_3$, TMS, ppm δ) 1.05–1.95 (16 protons, $(CH_2)_7$, m), 3.68 (2 protons, CH_2O, t), 4.01 (3 protons, OCH=CH_2 trans and $PhOCH_2$, m), 4.13 and 4.22 (1 proton, OCH=CH_2 cis, d), 6.50 (1 proton, OCH=CH_2, q), 7.02 (2 aromatic protons, ortho to alkoxy, d), 7.56 (2 aromatic protons, meta to alkoxy, d), 7.69 (4 aromatic protons, ortho and meta to CN, d of d).

Synthesis of 9-[(4-Cyano-4′-biphenylyl)oxy]nonyl Ethyl Ether (8–9). 4-Cyano-4′-[(9-hydroxynonan-1-yl)oxy]biphenyl (0.5 g, 1.48 mmol) was added to a solution containing potassium *tert*-butoxide (0.166 g, 1.48 mmol), a catalytic amount of 18-crown-6, and dry tetrahydrofuran (10 mL). Diethyl sulfate (0.197 mL, 1.5 mmol) was added and the reaction mixture was refluxed for 4 h under argon. After it cooled, the reaction mixture was poured into chloroform. The chloroform solution was extracted with 10% aqueous KOH, washed with water, and dried over magnesium sulfate and the solvent was removed in a rotavapor. The resulting product was purified by column chromatography (silica gel, CH_2Cl_2 eluent) and then was recrystallized from methanol to yield 0.32 g (59.2%) of white crystals. Purity, 99% (HPLC); mp 75.4 °C (DSC); ^{1}H NMR ($CDCl_3$, TMS, ppm) δ 1.19

Table I
Cationic Polymerization of 9-[(4-Cyano-4'-biphenylyl)oxy]nonyl Vinyl Ether (6-9)[a] and Characterization of the Resulting Polymers[b]

			GPC			phase transitions, °C (corresponding enthalpy changes, kcal/mru)	
sample	$[M]_0/[I]_0$	polym yield, %	$10^{-3}M_n$	M_w/M_n	DP	heating	cooling
1	2.0	44.2	0.9	1.54	3.0	g −1.6 s_A 104.1 (0.70) i g −1.6 s_A 103.8 (0.71) i	i 100.3 (0.71) s_A −6.7 g
2	4.0	31.0	1.8	1.13	5.0	g 5.8 s_A 120.6 (0.67) i g 5.0 s_A 120.2 (0.70) i	i 114.7 (0.69) s_A 0.8 g
3	6.0	55.9	2.0	1.24	6.0	g 11.7 s_A 125.1 (0.60) i g 9.2 s_A 124.4 (0.64) i	i 119.7 (0.64) s_A 3.3 g
4	8.0	61.6	2.9	1.07	8.0	g 10.1 s_A 131.8 (0.64) i g 9.4 s_A 131.9 (0.65) i	i 124.3 (0.63) s_A 4.2 6
5	10.0	68.0	3.8	1.20	10.0	g 12.0 s_A 135.9 (0.62) i g 11.1 s_A 135.9 (0.63) i	i 130.0 (0.63) s_A 5.0 g
6	13.0	63.3	4.5	1.20	12.0	g 13.3 s_A 141.5 (0.62) i g 12.5 s_A 141.0 (0.60) i	i 136.7 (0.61) s_A 7.5 g
7	18.0	65.3	5.9	1.28	16.0	g 13.3 s_A 144.7 (0.62) i g 12.7 s_A 144.7 (0.62) i	i 138.7 (0.61) s_A 7.5 g
8	23.0	69.3	8.4	1.16	22.0	g 13.8 s_A 149.9 (0.60) i g 13.0 s_A 150.7 (0.59) i	i 145.8 (0.59) s_A 9.8 g
9	30.0	74.3	11.6	1.12	32.0	g 14.2 s_A 153.8 (0.62) i g 14.2 s_A 153.6 (0.59) i	i 149.0 (0.58) s_A 10.0 g

[a] Polymerization temperature, 0 °C; polymerization solvent, methylene chloride; $[M]_0 = 0.275$; $[(CH_3)_2S]_0/[I]_0 = 10$; polymerization time, 1 h. [b] Data on the first line are from first heating and cooling scans. Data on the second line are from the second heating scan. The biphasic domain of the isotropization temperature is 11 ± 3 °C. The accuracy of M_w/M_n is ±0.01.

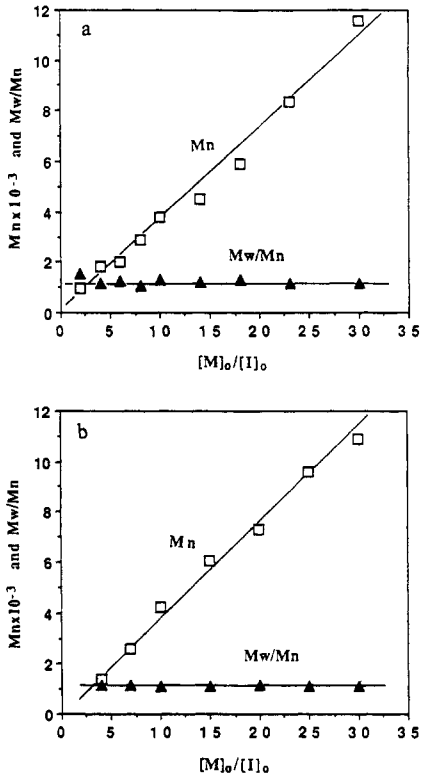

Figure 1. Dependence of the number-average molecular weight (M_n) and the polydispersity (M_w/M_n) of poly(6-9) (a) and poly(6-10) (b) on the $[M]_0/[I]_0$ ratio.

(3 protons, OCH_2CH_3, t), 1.29–1.98 (14 protons, $(CH_2)_7$, m), 3.40 (4 protons, $CH_2OCH_2CH_3$, m), 4.01 (2 protons, $PhOCH_2$, t), 7.01 (2 aromatic protons, ortho to alkoxy, d), 7.50 (2 aromatic protons, meta to alkoxy, d), 7.65 (4 aromatic protons, ortho and meta to CN, d of d).

Synthesis of 4-Cyano-4'-[(10-hydroxydecan-1-yl)oxy]biphenyl (7-10). 4-Cyano-4'-hydroxybiphenyl (3.9 g, 0.02 mol), potassium hydroxide (1.12 g, 0.02 mol), and a few crystals of potassium iodide were dissolved in a mixture of ethanol/water (7/3) (141.5 mL). 10-Bromodecan-1-ol (5 g, 0.21 mol) was added to the resulting solution, which was heated to reflux for 24 h. After it cooled, the mixture was poured into water and then filtered. The obtained solid was recrystallized from methanol and then benzene, to yield 4.1 g (58.3%) of white crystals. MP 97.4 °C (DSC); ^{1}H NMR ($CDCl_3$, TMS, ppm) δ 1.02–1.93 (16 protons, $(CH_2)_8$, m), 3.65 (2 protons, CH_2OH, t), 4.01 (2 protons, $PhOCH_2$, t), 7.02 (2 aromatic protons, ortho to alkoxy, d), 7.51 (2 aromatic protons, meta to alkoxy, d), 7.66 (4 aromatic protons ortho and meta to CN, d of d).

Synthesis of 10-[(4-Cyano-4'-biphenylyl)oxy]decanyl Vinyl Ether (6-10). 4-Cyano-4'-[(10-hydroxydecan-1-yl)oxy]biphenyl (1.50 g, 4.27 mmol) was added to a mixture of (1,10-phenanthroline)palladium(II) diacetate (0.17 g, 0.42 mmol), *n*-butyl vinyl ether (23.3 mL), and dry chloroform (18 mL). The mixture was heated to 60 °C for 6 h. After the mixture cooled, it was filtered to remove the catalyst and the solvent was distilled in a rotavapor. The product was purified by column chromatography (silica gel, CH_2Cl_2 eluent) and then recrystallized from *n*-hexane to yield 1.2 g (74.7%) of white crystals. Purity, 99.9% (HPLC); mp 65.4 °C, T_{n-i}, 69.8 °C (DSC); ^{1}H NMR ($CDCl_3$, TMS, ppm) δ 1.02–1.93 (16 protons, $(CH_2)_8$, m), 3.67 (2 protons, CH_2O, t), 4.01 (3 protons, $OCH{=}CH_2$ trans and $PhOCH_2$, m), 4.14 and 4.20 (1 proton, $OCH{=}CH_2$ cis, d), 6.49 (1 proton, $OCH{=}CH_2$, q), 7.01 (2 aromatic protons, ortho to alkoxy, d), 7.50 (2 aromatic protons, meta to alkoxy, d), 7.65 (4 aromatic protons, ortho and meta to CN, d of d).

Synthesis of 10-[(4-Cyano-4'-biphenylyl)oxy]decanyl Ethyl Ether (8-10). 4-Cyano-4'-[(10-hydroxydecan-1-yl)oxy]biphenyl (0.3 g, 0.85 mmol) was added to a solution containing potassium *tert*-butoxide (0.096 g, 0.85 mmol), a catalytic amount of 18-crown-6, and dry tetrahydrofuran (10 mL). Diethyl sulfate (0.114 mL, 0.94 mmol) was added and the reaction mixture was refluxed for 4 h under argon. After it cooled, the reaction mixture was poured into chloroform. The chloroform solution was extracted with 10% aqueous KOH, washed with water, and dried over magnesium sulfate and the solvent was removed in a rotavapor. The resulting product was purified by column chromatography (silica gel, CH_2Cl_2 eluent) and then was recrystallized from methanol to yield 0.23 g (54.2%) of white crystals. Purity, 99% (HPLC); mp 69.1 °C (DSC); ^{1}H NMR ($CDCl_3$, TMS, ppm) δ 1.20 (3 protons, OCH_2CH_3, t), 1.30–1.93 (16 protons, $(CH_2)_8$, m), 3.41 (4 protons, $CH_2OCH_2CH_3$, m), 4.01 (2 protons, $PhOCH_2$, t), 7.02 (2 aromatic protons, ortho to alkoxy, d), 7.51 (2 aromatic protons, meta to alkoxy, d), 7.66 (4 aromatic protons, ortho and meta to CN, d of d).

Cationic Polymerizations. Polymerizations were carried out in glass flasks equipped with Teflon stopcocks and rubber septa under argon atmosphere at 0 °C for 1 h. All glassware was dried overnight at 130 °C. The monomer was further dried under vacuum overnight in the polymerization flask. Then the flask was filled with argon and cooled to 0 °C and the methylene chloride, dimethyl sulfide, and triflic acid were added via a syringe.

Table II
Cationic Polymerization of 10-[(4-Cyano-4'-biphenylyl)oxy]decanyl Vinyl Ether (6–10)[a] and Characterization of the Resulting Polymers[b]

			GPC			phase transitions, °C (corresponding enthalpy changes, kcal/mru)	
sample	$[M]_0/[I]_0$	polym yield, %	$10^{-3}M_n$	M_w/M_n	DP	heating	cooling
1	4	71.3	1.40	1.15	4.0	g 3.6 k 51.1 (3.77) s_A 116.6 (0.83) i g 0.0 s_A 115.9 (0.86) i	i 110.9 (0.82) s_A −5.5 g
2	7	66.0	2.60	1.13	7.0	g 8.7 k 49.7 (2.70) s_A 128.1 (0.78) i g 2.7 s_A 127.6 (0.80) i	i 122.0 (0.79) s_A −0.1 g
3	10	78.0	4.20	1.08	11.0	g 11.8 k 53.4 (2.34) s_A 139.5 (0.77) i g 6.4 s_A 138.6 (0.76) i	i 132.4 (0.74) s_A 2.7 g
4	15	74.0	6.10	1.09	16.0	g 12.7 k 53.8 (2.68) s_A 147.0 (0.78) i g 14.8 s_X 37.0 (0.62) s_A 147.8 (0.76) i	i 142.9 (0.73) s_A 24.9 (0.58) s_X 9.8 g
5	20	84.7	7.30	1.14	19.0	g 15.5 k 55.0 (2.39) s_A 153.7 (0.76) i g 16.2 s_X 44.9 (0.68) s_A 152.9 (0.74) i	i 147.3 (0.72) s_A 37.4 (0.80) s_X 11.8 g
6	25	82.7	9.60	1.10	25.0	g 16.2 k 55.2 (2.35) s_A 155.2 (0.75) i g 16.0 s_X 48.2 (0.69) s_A 154.1 (0.72) i	i 149.1 (0.71) s_A 41.8 (0.84) s_X 12.2 g
7	30	73.3	10.90	1.09	28.0	g 17.4 k 56.1 (2.35) s_A 156.5 (0.78) i g 16.5 s_X 50.6 (0.91) s_A 157.0 (0.71) i	i 151.2 (0.70) s_A 44.1 (0.84) s_X 12.8 g

[a] Polymerization temperature, 0 °C; polymerization solvent, methylene chloride; $[M]_0 = 0.265$; $[(CH_3)_2S]_0/[I]_0 = 10$; polymerization time, 1 h. [b] Data on first line are from first heating and cooling scans. Data on the second line are from the second heating scan. The biphasic domain of the isotropization temperature is 11 ± 3 °C. The accuracy of M_w/M_n is ±0.01.

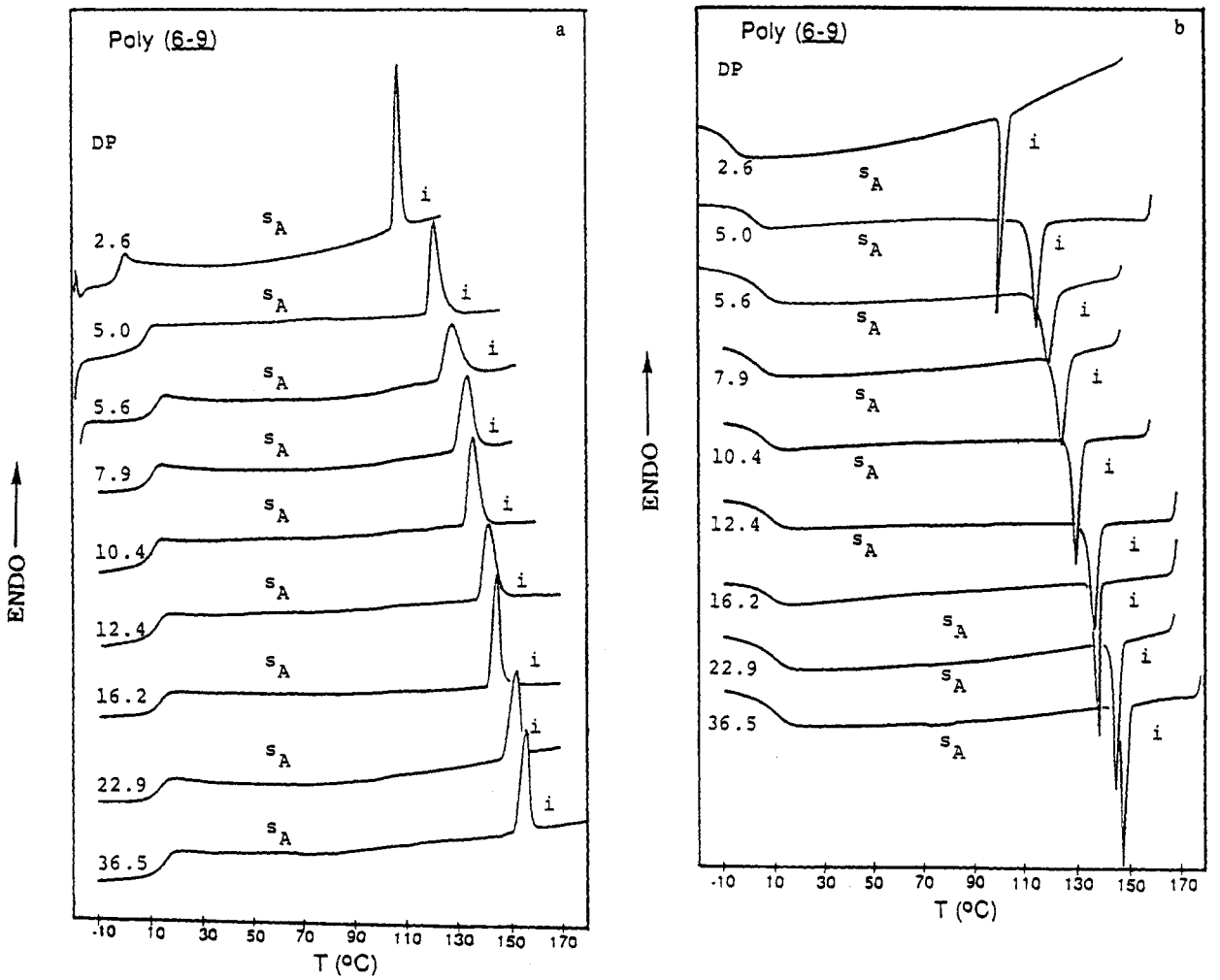

Figure 2. DSC traces displayed during the second heating scan (a) and first cooling scan (b) by poly(6–9) with different degrees of polymerization (DP). The DP is printed on the top of each DSC scan.

The monomer concentration was about 10 wt % of the solvent volume and the dimethyl sulfide concentration was 10 times larger than that of the initiator. The polymer molecular weight was controlled by the monomer/initiator ($[M]_0/[I]_0$) ratio. After quenching the polymerization with ammoniacal methanol, the reaction mixture was precipitated into methanol. The filtered polymers were dried and precipitated from methylene chloride solutions into methanol until GPC traces showed no traces of monomer. Tables I and II summarize the polymerization results. Although polymer yields are lower than expected due to losses during the purification process, conversions were almost quantitative in all cases.

Table III
Thermal Characterization of 4-Cyano-4'-[(ω-hydroxyalkan-1-yl)oxy]biphenyls 7–9 and 7–10, ω-[(4-Cyano-4'-biphenylyl)oxy]alkyl Vinyl Ethers 6–9 and 6–10, and ω-[(4-Cyano-4'-biphenylyl)oxy]alkyl Ethyl Ethers 8–9 and 8–10

	phase transitions, 0 °C (corresponding enthalpy changes, kcal/mol)	
compd	heating[a]	cooling[b]
7–9	k 81.4 (9.10) n 98.9 (0.34) i	i 96.0 (0.35) n 54.9 (6.45) k
6–9	k 63.1 (10.20) i [n 59.2 (0.36) i]	i 56.2 (0.33 n 28.9 (7.31) k
8–9	k 75.4 (10.22) i	i 53.2 (0.29) n 50.3 (—)* s_A 41.3 (8.23)* k
7–10	k 97.4 (10.0) i [n 97.2 (0.45) i]	i 94.2 (0.52) n 75.5 (8.3) k
6–10	k 65.4 (8.4) n 69.8 (0.36) i]	i 66.1 (0.43) n 52.6 (8.19) k
8–10	k 69.1 (12.9) i [s_A 65.0 (0.71)]	i 57.1 (0.72) s_A 27.9 (8.66) k

[a] [ ], virtual data. [b] *, overlapped peaks.

Results and Discussion

The results of the cationic polymerization of 6–9 and 6–10 are summarized in Tables I and II. The molecular weights of both poly(6–10) and poly(6–10) were controlled by varying the ratio $[M]_0/[I]_0$. As mentioned in the Experimental Section, the yields reported in Tables I and II are below 100%. This is due to polymer loss during the purification process. However, conversions are quantitative. Both the number-average molecular weight (M_n) and M_w/M_n exhibit a linear dependence on $[M]_0/[I]_0$. The plots of these dependences are shown in Figure 1 and demonstrate that both monomers 6–9 and 6–10 polymerize through a living mechanism.

Table III summarizes the phase transition temperatures of 4-cyano-4'-[(ω-hydroxyalkan-1-yl)oxy]biphenyls (7–9 and 7–10), ω-[(4-cyano-4'-biphenylyl)oxy]alkyl vinyl ethers (6–9 and 6–10), and ω-[(4-cyano-4'-biphenylyl)oxy]-alkyl ethyl ethers (8–9 and 8–10). They were determined by a combination of DSC and thermal optical polarized microscopy techniques. The difference between the phase behavior of 7–9, 6–9, and 8–9 is determined by the functional group attached to the end of the alkyl unit. As we can observe from the data summarized in Table III, on going from 7–9 to 6–9 to 8–9 the mesomorphic behavior of the compound changes from enantiotropic nematic to monotropic nematic to a combination of monotropic nematic and smectic A (s_A). This trend is different for the same series of compounds containing a decanyl alkyl group. Thus 7–10 and 8–10 exhibit a monotropic nematic and a monotropic smectic A mesophase, respectively, while 6–10 exhibits an enantiotropic nematic mesophase. Of general interest for the discussion that follows is the phase behavior of 8–9 and 8–10, which are the model compounds of the monomeric structural units of poly(6–9) and poly(6–10). In other words, 8–9 and 8–10 represent poly(6–9) and poly(6–10) with degrees of polymerization equal to one.

Heating and cooling DSC traces of poly(6–9) with degrees of polymerization from about 2.0–32.0 are presented in Figure 2. The heating DSC scans are identical irrespective of the thermal history of the sample. Therefore, first, second, and subsequent heating scans are identical. The DSC traces obtained from the second heating and first cooling scans are exhibited in Figure 2. However, data collected from both first and second heating scans are presented in Table I and plotted in Figure 3a. The phase transition temperatures determined from the cooling scan are plotted in Figure 3b. Over the entire range of molecular weights, poly(6–9) displays only an

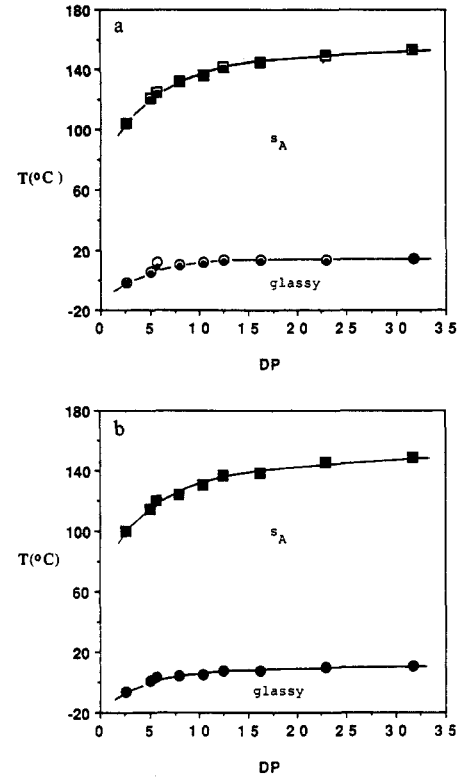

Figure 3. Dependence of phase transition temperatures on the degree of polymerization of poly(6–9). (a) Data from the first heating (fh) and the second heating scans (sh): ○, T_g (fh); □, T_{s_A-i} (fh); ●, T_g (sh); ■, T_{s_A-i} (sh). (b) Data from the first cooling scan: ■, T_{i-s_A}; ●, T_g.

enantiotropic s_A mesophase. This mesophase exhibits a classic focal conic fan-shaped texture. As we have discussed at the beginning of this section, 8–9 displays both nematic and monotropic s_A mesophases. Since poly(6–9) with a degree of polymerization of about three shows only an enantiotropic s_A phase, this means that the slope of the T_{n-s_A}–M_n dependence is higher than that of the T_{n-i}–M_n dependences. The intercept of these two dependences occurs below the point where poly(6–9) reaches a degree of polymerization equal to three. A dependence like this, which, however, was expanding over a larger range of molecular weights, was observed for both poly(6–6) and poly(6–8).[12] The overall behavior of poly(6–9) is of interest since this polymer does not present side-chain crystallization at any molecular weight (Figure 3).

The DSC traces of poly(6–10) obtained from the first and second heating and from the first cooling scans are presented in Figure 4. Poly(6–10) presents a mesomorphic behavior which resembles that of poly(6–11).[11] The first and second DSC heating scans of poly(6–10) are different and, therefore, both are shown in Figure 4a,b. In the first DSC heating scan, poly(6–10)s exhibit a crystalline melting followed by an enantiotropic s_A mesophase (Figure 4a). In the first cooling scan, poly(6–10)s with degree of polymerization up to 16 exhibit the transition from the isotropic to the s_A phase followed by a glass transition temperature (Figure 4c). Poly(6–10)s with higher degrees of polymerization exhibit the transition from the isotropic to the s_A followed by a transition from the s_A to a s_X (unidentified smectic phase). On the subsequent heating (Figure 4b) and cooling (Figure 4c) scans, depending on the degree of polymerization, poly(6–10) exhibits either an enantiotropic s_A or enantiotropic s_A and s_X phases (Table II). However, if we anneal the polymer sample above the glass transition temperature after cooling and reheating, side-chain crystallization

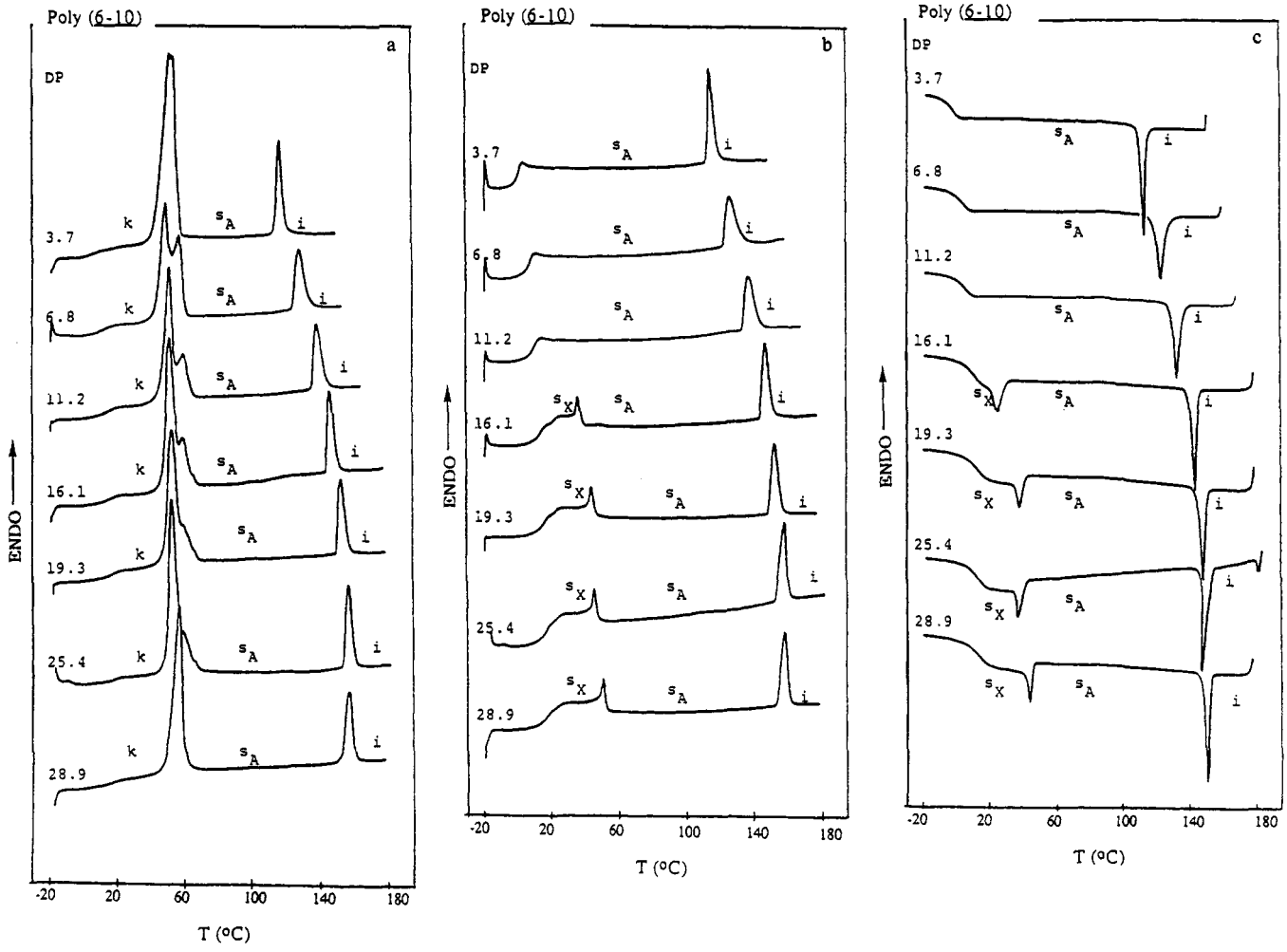

Figure 4. DSC traces displayed during the first heating scan (a), the second heating scan (b), and the first cooling scan (c) by poly(6–10) with different degrees of polymerization (DP). The DP is printed on the top of each DSC scan.

occurs again and the polymer exhibits the same DSC heating scan as the first heating scan (Figure 4a).

The thermal behavior of poly(6–10) is very similar to that of poly(6–11).[11] The dependence of molecular weight of the mesomorphic behavior of poly(6–10) is plotted in Figure 5a for the first heating scan, in Figure 5b for the second and subsequent heating scans, and in Figure 5c for the first and subsequent cooling scans.

Let us now compare the phase behavior of poly(6–*n*) with n = 2–11 at four different degrees of polymerization: 30, 23, 13, and 4. Figure 6 presents the thermal transition temperatures determined from the second heating scan, while Figure 7 presents the same thermal transition temperatures determined from the first heating scan. Thermal transition temperatures of poly(6–9) and poly(6–10) were determined in this paper. The results of poly(6–2), poly(6–3), and poly(6–4),[14] poly(6–5) and poly(6–7),[15] poly(6–6) and poly(6–8),[12] and poly(6–11)[11] were reported in previous publications from this series.

Figure 6a,b presents the thermal transitions, determined from second heating scans of poly(6–*n*), with degrees of polymerization of 30 and 23. Both plots demonstrate the same trend. Glass transition temperatures of poly(6–*n*) decrease with the increase of the polymer spacer length. Poly(6–2) with a degree of polymerization of 30 does not exhibit any mesophase. Poly(6–3) and poly(6–4) display a nematic mesophase, while poly(6–5) a s_A and a nematic mesophase. Poly(6–6), poly(6–8), poly(6–10), and poly(6–11) exhibit a s_X (an unidentified smectic mesophase) and a s_A mesophase. The isotropization transition temperature increases with the increase of the spacer length. Upon decreasing the degree of polymeriazation, all phase transition temperatures of poly(6–*n*) decreased.

For polymers with short spacers, the isotropization temperature seems to follow an odd–even effect that is opposite to that observed in the case of main-chain liquid crystalline polymers containing flexible spacers.[23] That is, in the case of side-chain liquid crystalline polymers the highest isotropization temperature is exhibited by the polymers containing odd spacers, while in the case of main-chain liquid crystalline polymers it is shown by the polymers containing even spacers.[23] A similar behavior was observed in the case of side-chain liquid crystalline polymethacrylates based on cyanobenzoyl ester and cyanophenyl ester mesogens and various spacer lengths.[24,25] These data, together with those of various polymers containing 4-cyanobiphenyl and other mesogenic side groups with different spacer lengths and polymer backbones, seem to indicate the same trend and are discussed in a recent review article.[1]

Let us now compare the phase behavior of poly(6–*n*) with degrees of polymerization 30 and 23, determined from second heating scan, with that determined from the first heating scans. Data collected from first heating scans are presented in Figure 7a,b. With the exception of poly(6–2), the nature of the highest temperature mesophase of all polymers is identical, regardless of the scan it was collected from. In the first heating scan, poly(6–2) exhibits a s_X mesophase. A s_X mesophase is also observed in the first heating scan of poly(6–3) and poly(6–4). In the first heating scan, poly(6–10) and poly(6–11) exhibit a crys-

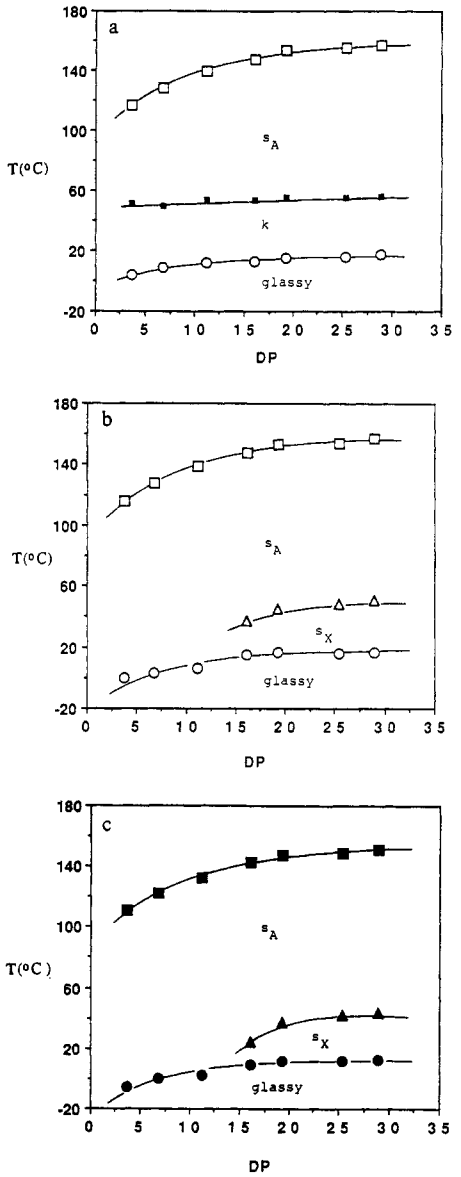

Figure 5. Dependence of phase transition temperatures on the degree of polymerization of poly(6–10). (a) Data from the first heating scan: ○, T_g; ■, T_{k-s_A}; □, T_{s_A-i}. (b) Data from the second heating scan: ○, T_g; △, $T_{s_X-s_A}$; □, T_{s_A-i}. (c) Data from the first cooling scan: ■, T_{i-s_A}; ▲, $T_{s_A-s_X}$; ●, T_g.

talline phase, while in their second heating scan they exhibit a s_X phase.

Upon decreasing the degree of polymerization from 23 to 13, the phase behavior of poly(6–4) changes even more (Figure 6b,c). On the second heating scan, the highest temperature mesophases of poly(6–*n*)s with degree of polymerization 13 are identical with those of the corresponding polymers with degree of polymerization 13 are identical with those of the corresponding polymers with degree of polymerization 23. However, with the exception of poly(6–5), no second mesophase is observed in the case of polymers with degree of polymerization of 13 (see part c versus b in Figure 6). In the first heating scan, a mesophase or crystalline phase is observed for the polymers with degrees of polymerization 13 (Figures 7c and 6c). Poly(6–*n*)s with degrees of polymerization of 4 exhibit an even more drastic change of their phase behavior, particularly in the case of polymers with short flexible spacers. Thus, in the second heating scan, poly(6–2) with a degree of polymerization of 4 exhibits a nematic phase, while in the first heating scan it exhibits a s_X and a nematic phase. Poly(6–3), poly(6–4), poly(6–5), and poly(6–6) display a

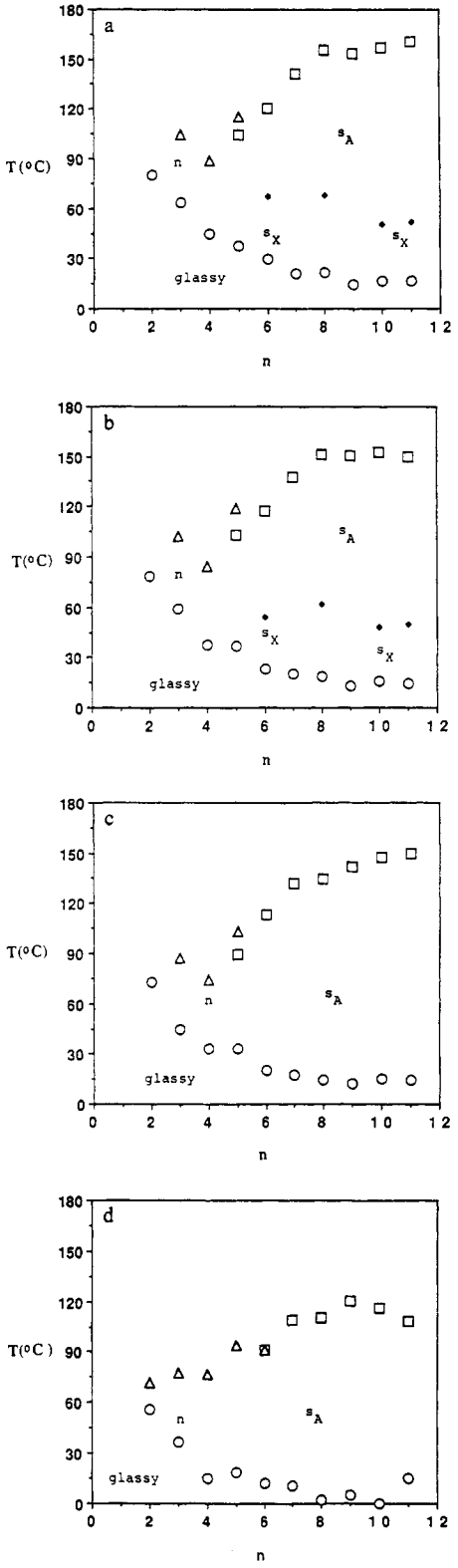

Figure 6. Dependence of phase transition temperatures on the length (*n*) of the flexible spacer [–$(CH_2)_n$–] of poly(6–*n*) at similar degrees of polymerization. (a) Data from the second heating scan at DP = 30: ○, T_g; ♦, $T_{s_X-s_A}$; □, T_{s_A-i}; △, T_{n-i}. (b) Data from the second heating scan at DP = 23: ○, T_g; ♦, $T_{s_X-s_A}$; □, T_{s_A-i}; △, T_{n-i}. (c) Data from the second heating scan at DP = 13: ○, T_g; □, T_{s_A-i}; △, T_{n-i}. (d) Data from the second heating scan at DP = 4: ○, T_g; □, T_{s_A-i}; △, T_{n-i}.

nematic phase both in the second and first heating scans (Figures 6d and 7d). In both the second and first heating scans, poly(6–6) with degree of polymerization 4 shows a s_A and a nematic phase, which overlap each other. The main difference between the first and second heating scans

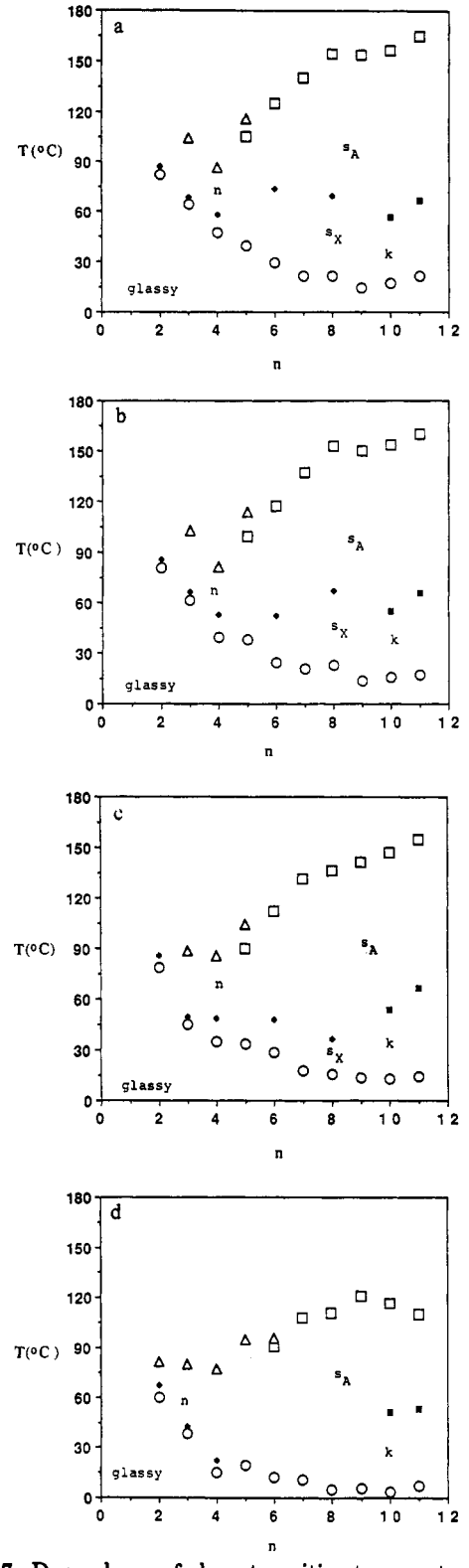

Figure 7. Dependence of phase transition temperatures on the length (n) of the flexible [$-(CH_2)_n-$] spacer of poly(6-n) at similar degrees of polymerization. (a) Data from the first heating scan at DP = 30: ○, T_g; ‖, $T_{s_X-s_{A(n)}}$; ■, T_{k-s_A}; □, T_{s_A-i}; △, T_{n-i}. (b) Data from the first heating scan at DP = 23: ○, T_g; ♦, $T_{s_X-s_{A(n)}}$; ■, T_{k-s_A}; □, T_{s_A-i}; △, T_{n-i}. (c) Data from the first heating scan at DP = 13: ○, T_g; ♦, $T_{s_X-s_{A(n)}}$; ■, T_{k-s_A}; □, T_{s_A-i}; △, T_{n-i}. (d) Data from the first heating scan at DP = 4: ○, T_g; ♦, T_{s_X-n}; ■, T_{k-s_A}; □, T_{s_A-i}; △, T_{n-i}.

of the polymers with degrees of polymerization 4 is observed for poly(6-2), poly(6-3), poly(6-10), and poly(6-11), which, in addition to the phases exhibited in the second heating scan (Figure 6d), in the first heating scan present a s_X phase in the case of the first two polymers and a crystalline phase in the case of the last two polymers (Figure 7d).

As described in more detail in each particular case,[11-15,26,27] the experimental results summarized in Figures 6 and 7 can be explained at least in a qualitative way. There are two combined effects that determine the influence of polymer molecular weight on its phase transitions.

The first one is a thermodynanamic effect,[16,17] which through its entropic factor predicts that mesomorphic phase transition temperatures increase with the increase of the polymer molecular weight up to a certain value beyond which they remain constant. The T_g of the polymer exhibits the same trend. The slopes of dependences of various phase transitions versus molecular weight are spacer length dependent. Depending on the ratio between various slopes, a virtual phase transition may become enantiotropic either above or below a certain degree of polymerization. The first situation is representative for the s_X phase of poly(6-6), poly(6-8), poly(6-10), and poly(6-11), which becomes enantiotropic at high molecular weights (Figure 6a-c). The second situation is observed in the case of poly(6-2), which displays an enantiotropic nematic mesophase only at low molecular weights (Figure 6c,d). In this particular case, the slope of T_g-M_n dependence is steeper than that of the nematic-isotropic-M_n dependence and, therefore, at higher molecular weights this enantiotropic nematic phase becomes virtual.[14]

The second effect is a kinetic one. That is both liquid crystalline and crystalline phase transitions become kinetically controlled especially when they are in the close proximity of T_g and/or when the polymers have high molecular weights. This behavior is characteristic for the s_X phase of poly(6-2), poly(6-3), and poly(6-4) (Figure 7) (due to its close proximity to T_g) and for the crystalline phases of poly(6-10) and poly(6-11) (Figures 6 and 7).

The data reported in this series of publications on the influence of molecular weight on the phase behavior of poly{ω-[(4-cyano-4'-biphenylyl)oxy]alkyl vinyl ether}s provide the most comprehensive collection of results available to date on a polymer homologues series of side-chain liquid crystalline polymers. They are important since they can be used to tailer make novel macromolecular architectures based on side-chain liquid crystalline polymers, as well as to provide a theoretical explanation for the trends obtained from these experiments. The first series of experiments on statistical binary copolymers with well-defined composition, molecular weight, and molecular weight distribution, prepared by living carbocationic copolymerization, have already been reported.[26,27] By analogy with the case of main-chain liquid crystalline copolymers,[23,28,29] it has been demonstrated that the isomorphism of the structural units of the copolymer is determining the mesomorphic behavior of side-chain liquid crystalline copolymers.[26,27] Since the phase behavior of poly(6-n)s is molecular weight dependent, the mesomorphic behavior of statistical copolymers based on various pairs of 6-n is also molecular weight dependent. Experiments on the molecular engineering of both statistical and sequential copolymers are in progress and will be reported in due time.

Acknowledgment. Financial support from the Office of Naval Research is gratefully acknowledged.

References and Notes

(1) Percec, V.; Pugh, C. In *Side Chain Liquid Crystal Polymers*; McArdle, C. B., Ed.; Chapman and Hall: New York, 1989; p 30 and references cited therein.

(2) Kostromin, S. G.; Talroze, R. V.; Shibaev, V. P.; Plate, N. A. *Makromol. Chem., Rapid Commun.* **1982**, *3*, 803.
(3) Stevens, H.; Rehage, G.; Finkelmann, H. *Macromolecules* **1984**, *17*, 851.
(4) Shibaev, V. *Mol. Cryst. Liq. Cryst.* **1988**, *155*, 189.
(5) Uchida, S.; Morita, K.; Miyoshi, K.; Hashimoto, K.; Kawasaki, K. *Mol. Cryst. Liq. Cryst.* **1988**, *155*, 93.
(6) Percec, V.; Hahn, B. *Macromolecules* **1989**, *22*, 1588.
(7) Percec, V.; Tomazos, D.; Pugh, C. *Macromolecules* **1989**, *22*, 3259.
(8) Sagane, T.; Lenz, R. W. *Polym. J.* **1988**, *20*, 923.
(9) Sagane, T.; Lenz, R. W. *Polymer* **1989**, *30*, 2269.
(10) Sagane, T.; Lenz, R. W. *Macromolecules* **1989**, *22*, 3763.
(11) Percec, V.; Lee, M.; Jonsson, H. *J. Polym. Sci., Polym. Chem. Ed.* **1991**, *29*, 327.
(12) Percec, V.; Lee, M. *Macromolecules* **1991**, *24*, 1017.
(13) Percec, V.; Lee, M. *Polym. Bull.* **1991**, *25*, 123.
(14) Percec, V.; Lee, M. *J. Macromol. Sci., Chem. Ed.*, in press.
(15) Percec, V.; Lee, M. *Polymer*, in press.
(16) Percec, V.; Keller, A. *Macromolecules* **1990**, *23*, 4347.
(17) Keller, A.; Ungar, G.; Percec, V. In *Advances in Liquid Crystalline Polymers*; Weiss, R. A., Ober, C. K., Eds.; ACS Symposium Series 435; American Chemical Society: Washington, DC, 1990; p 308.
(18) Cho, C. G.; Feit, B. A.; Webster, O. W. *Macromolecules* **1990**, *23*, 1918.
(19) Demus, D.; Richter, L. *Textures of Liquid Crystals*; Verlag Chemie: Weinheim, 1978.
(20) Gray, G. W.; Goodby, J. W. *Smectic Liquid Crystals. Textures and Structures*; Leonard Hill: Glasgow, 1984.
(21) McKeon, J. E.; Fitton, P. *Tetrahedron* **1972**, *28*, 223.
(22) Rodenhouse, R.; Percec, V.; Feiring, A. E. *J. Polym. Sci., Part C: Polym. Lett.* **1990**, *28*, 345.
(23) Percec, V.; Tsuda, Y. *Macromolecules* **1990**, *23*, 3509.
(24) Mauzac, M.; Hardouin, F.; Richard, H.; Achard, M. F.; Sigaud, G.; Gasparoux, H. *Eur. Polym. J.* **1986**, *22*, *137*.
(25) Gemmel, D. A.; Gray, G. W.; Lacey, D. *Mol. Cryst. Liq. Cryst.* **1985**, *122*, 205.
(26) Percec, V.; Lee, M. *Polymer*, in press.
(27) Percec, V.; Lee, M. *Polym. Bull.* **1991**, *25*, 131.
(28) Percec, V.; Tsuda, Y. *Macromolecules* **1990**, *23*, 5.
(29) Percec, V.; Tsuda, Y. *Polymer* **1991**, *32*, 661 and 673.

Registry No. **6–9**, 132981-36-3; **6–9** (homopolymer), 132981-40-9; **6–10**, 132981-39-6; **6–10** (homopolymer), 132981-41-0; **7–9**, 132981-35-2; **7–10**, 132981-38-5; **8–9**, 132981-37-4; **8–10**, 133008-43-2; $HO(C_6H_4\text{-}p)_2CN$, 19812-93-2; $Br(CH_2)_9OH$, 55362-80-6; $BuOCH{=}CH_2$, 111-34-2; $Br(CH_2)_9OH$, 53463-68-6; diethyl sulfate, 64-67-5.